

See discussions, stats, and author profiles for this publication at: <https://www.researchgate.net/publication/221804669>

Sided Functions of an Arginine–Agmatine Antiporter Oriented in Liposomes

ARTICLE *in* BIOCHEMISTRY · FEBRUARY 2012

Impact Factor: 3.02 · DOI: 10.1021/bi201897t · Source: PubMed

CITATIONS

5

READS

29

3 AUTHORS, INCLUDING:



Ming-Feng Tsai

Brandeis University

10 PUBLICATIONS 130 CITATIONS

[SEE PROFILE](#)



Christopher Miller

Brandeis University

107 PUBLICATIONS 3,052 CITATIONS

[SEE PROFILE](#)



NIH Public Access

Author Manuscript

Biochemistry. Author manuscript; available in PMC 2013 February 28.

Published in final edited form as:
Biochemistry. 2012 February 28; 51(8): 1577–1585. doi:10.1021/bi201897t.

Sided functions of an arginine-agmatine antiporter oriented in liposomes

Ming-Feng Tsai, Yiling Fang, and Christopher Miller

Department of Biochemistry, Howard Hughes Medical Institute, Brandeis University, Waltham, Massachusetts 02454

Abstract

The arginine-dependent extreme acid resistance system helps enteric bacteria survive the harsh gastric environment. At the center of this multi-protein system is an arginine-agmatine antiporter, AdiC. To maintain cytoplasmic pH, AdiC imports arginine and exports its decarboxylated product agmatine, resulting in a net extrusion of one “virtual proton” in each turnover. The random orientation of AdiC in reconstituted liposomes throws up an obstacle to quantifying its transport mechanism. To overcome this problem, we introduced a mutation, S26C, near the substrate-binding site. This mutant exhibits similar substrate recognition and pH-dependent activity as wild-type protein, but loses function completely upon reaction with thiol reagents. The membrane-impermeant MTSES reagent can then be used as a cleanly sided inhibitor to silence those S26C-AdiC proteins whose extracellular portion projects from the external side of the liposome. Alternatively, the membrane-permeant MTSEA and membrane-impermeant reducing reagent, TCEP, can be used together to inhibit proteins in the opposite orientation. This approach enables steady-state kinetic analysis of AdiC in a sided fashion. Arginine and agmatine have similar Michaelis-Menten parameters for both sides of the protein, while the extracellular side selects arginine over argininamide, a mimic of the carboxylate-protonated form of arginine, more effectively than does the cytoplasmic side. Moreover, the two sides of AdiC have different pH-sensitivities. AdiC activity increases to a plateau at pH 4 as the extracellular side is acidified, while the cytoplasmic side shows an optimal pH of 5.5, with further acidification inhibiting transport. This oriented system allows more precise analysis of AdiC-mediated substrate transport than has been previously available and permits comparison to the situation experienced by the bacterial membrane under acid stress.

From the viewpoint of enteric bacteria, the mammalian stomach, where pH can fall as low as 1.5, is a potentially lethal barrier that must be surmounted to colonize the intestinal tract. Many bacteria breach this host defense by activating multiple extreme acid resistance (XAR) systems (1, 2). This study concerns one of these, the arginine-dependent XAR system, which is composed of an arginine-agmatine antiporter, AdiC, and an acid-activated arginine decarboxylase, AdiA (3, 4). To counter acidification of the cytosol during low pH exposure, AdiC imports arginine, which is then decarboxylated by AdiA; this reaction consumes an aqueous proton, which replaces the α -carboxyl of arginine to form agmatine (1-amino-4-guanidino-n-butane). Agmatine is then exported by the same transporter, resulting in net extrusion of one “virtual proton” (5) from the cytosol in each AdiC transport cycle (Fig. 1A).

Corresponding author: Christopher Miller, cmiller@brandeis.edu, Phone: 781-7362340.

Supporting Information Available: Fig. S1, proton leakage through proteoliposomes; Fig. S2, the dose response of MTS reagents; Fig. S3, effects of MTSEA on the C-less mutant; Fig. S4, S26AAdiC: arginine binding and transport; Fig. S5, maximal activation of AdiC by acid stress. These materials are available free of charge via the Internet at <http://pubs.acs.org>.

Previous studies have revealed basic biochemical, functional, and structural characteristics of AdiC (6–9). The protein is a homodimer in which each subunit acts as a self-contained antiporter that mediates strict one-to-one exchange of arginine for agmatine and is activated by low pH. AdiC's detailed transport mechanism, however, remains unclear. Several central questions are yet to be answered, including how AdiC senses pH changes and how it avoids transporting the protonated-carboxylate form of the substrate, Arg²⁺, the predominant form of arginine below pH 2.3, as it must do to achieve acid-resistance. Recent high-resolution structures of AdiC in multiple states (7–9) provide opportunities to tackle issues like these.

But crystal structures alone are not enough. Close analysis of transport mechanism requires reconstituting purified protein into liposomes for flux measurements. However, AdiC, like many membrane proteins, inserts into liposome membranes randomly, with two populations of protein oriented in opposite directions. This heterogeneous orientation is a severe impediment to examining a transport mechanism, since it precludes assignment of specific functions to defined sides of the protein and makes it impossible to obtain the protein's kinetic parameters in a quantitatively meaningful way. A method to orient AdiC in liposomes is therefore necessary for detailed mechanistic analysis. In some cases, oriented reconstituted systems may be achieved by the application of sided inhibitors, which exclusively silence one of the two protein populations present. However, no sided inhibitor of AdiC has yet been found.

Here, guided by crystal structures, we introduce an innocuous serine-to-cysteine substitution at a position that contributes to AdiC's arginine-binding site. This maneuver permits the use of thiol-directed methanethiosulfonate (MTS) reagents to inhibit AdiC in a strictly sided fashion, to yield liposomes with protein reconstituted in either of two orientations, outside-out or inside-out. An initial kinetic analysis reveals the sidedness of the protein's basic transport parameters, as well as the distinct pH-sensitivities of the cytoplasmic and extracellular sides. This work paves the way for future detailed examination of AdiC's transport mechanism and structural correlates thereof.

Materials and Methods

Chemical reagents

Lipids, including E. coli polar lipid (EPL), 1-palmitoyl-2-oleoyl phosphatidyl-ethanolamine (POPE), and 1-palmitoyl-2-oleoyl phosphatidylglycerol (POPG) were purchased from Avanti Polar Lipids. MTS reagents, 2-sulfonatoethyl methanethiosulfonate (MTSES) / 2-aminoethyl methanethiosulfonate (MTSEA), and detergents, including n-decylmaltofside (DM) and 3-[{3-cholamido-propyl}dimethylammonio]-1-propanesulfonate (CHAPS), were obtained from Anatrace. Tris(2-carboxyethyl)phosphine (TCEP) was purchased from Soltec Ventures, fluorescein-5-maleimide from Sigma-Aldrich, and ¹⁴C-arginine was from PerkinElmer. All other chemicals were of the highest grade available.

Protein expression and purification

The coding sequence of *Salmonella enterica* AdiC was inserted into the pASK-IBA2 vector between the XbaI and HindIII restriction sites (7). A thrombin-cleavable hexahistidine tag (HHHHHHSGGLVPRGSGT) was placed immediately after the initiator methionine to yield our working "wildtype" (WT) construct. Standard two-step PCR was used for site-directed mutagenesis, and full coding sequences were confirmed for all mutants. A cysteine-free AdiC, henceforth denoted "C-less," was constructed by substituting serine for the 8 native cysteines (positions 80, 98, 129, 238, 281, 286, 369, 398).

Detailed protein expression and purification procedures have been described (6). In brief, AdiC constructs were expressed in BL21 (DE3) cells, extracted in 40 mM DM, 100 mM

NaCl, 50 mM Tris-HCl, pH 8.0, and purified by cobalt-affinity (Talon) and size-exclusion columns (Superdex 200). For proteins with the S26C mutation, 2 mM TCEP was added after the extraction step to keep the introduced cysteine residue reduced. The final protein product was collected in 5 mM DM, 100 mM NaCl, 25 mM tris-HCl, pH 7.5, and concentrated to 10–20 mg/mL. The final yield was typically 10–15 mg for WT-AdiC or 5–10 mg for C-less mutants per liter of bacteria culture.

Isothermal titration calorimetry (ITC)

AdiC, concentrated to 100–300 μ M in 10–20 mM DM, was loaded into the 170- μ L sample cell (Nano-ITC, TA Instruments). After equilibration at 25 °C, arginine at 2–10 mM in the same solvent as the protein solution was titrated into the sample cell by 20–30 successive 1- μ L injections at 2–3-min intervals. Data were fit to single-site isotherms using software provided by the ITC manufacturer (NanoAnalyze 2.1.9). For experiments with MTSEA-modified protein, AdiC was treated with 5 mM MTSEA for 30 min and then repurified by size-exclusion chromatography.

Reconstitution of AdiC

Lipid (EPL or POPE:POPG 3:1, w/w, stored in chloroform at –80 °C) was dried under N₂, washed twice with pentane, and suspended to a final concentration of 20 mg/mL in reconstitution buffer (RB, 150 mM KCl, 25 mM citrate, KOH pH 5.5) with 35 mM CHAPS included. The suspension was sonicated to clarity, and AdiC was added to the desired concentration (5–10 μ g protein/mg lipid). The protein-detergent-lipid mixture was dialyzed overnight at 4 °C against RB supplemented with 1 mM TCEP, followed by two more 24-hr dialyses against fresh RB solution without TCEP. The resulting proteoliposomes, frozen in aliquots at –80 °C, remain fully functional for at least 6 months.

Arginine uptake assay

Proteoliposomes were prepared for arginine fluxes by adding 5 mM arginine to the liposome suspension, which was then subjected to 2–3 freeze-thaw cycles. After the final thawing step, liposomes were sonicated briefly, and extraliposomal arginine was removed by spinning 100- μ L aliquots through 1.5-mL Sephadex G-50 columns equilibrated with RB and dried by pre-spinning. Transport was initiated by adding 50 μ M ¹⁴C-arginine (1 μ Ci/mL). At desired time points, 50- μ L samples were loaded onto 2.2-mL Sephadex G-50 columns equilibrated with RB to terminate the uptake reaction. Liposomes were collected into scintillation vials by flushing the column with 1.6 mL RB. We frequently use fractional uptake” as a transport metric, defined as the fraction of total radioactivity that is trapped within the liposomes. This procedure was slightly modified to measure initial rates of arginine uptake. Instead of G-50 columns, 2.2-mL Dowex 50-X4 columns, N-methyl glucamine (NMG) form, equilibrated with RB was used to stop arginine uptake, a maneuver that shortens the system’s dead-time to ~5 s. After the 30-s uptake reaction, columns were flushed with 2 mL RB to collect liposomes into scintillation vials.

To gauge the pH-dependence of arginine transport with symmetrical pH 4 or 7, EPL proteoliposomes were prepared by dialyzing AdiC-lipid-detergent solution against 150 mM KCl buffered with either 25 mM succinate pH 4 or 25 mM MOPS pH 7. Arginine uptake was determined as above, except that these succinate or MOPS buffers were used rather than RB. For experiments with asymmetrical pH (5.5 inside / 3–8 outside), it was necessary to use POPE/POPG liposomes, as these, unlike EPL liposomes, are much less permeable to H⁺ on the uptake timescale (Fig. S1). After loading the liposomes with 5 mM arginine, the external solution was exchanged, as above, on G50 spin-columns equilibrated with 150 mM KCl, 1 mM citrate, pH 5.5. Immediately before starting the transport reaction, extraliposomal pH was altered by diluting the liposomes into 2.5 volumes of 150 mM KCl,

along with 25 mM of the appropriate buffer: citrate for pH 3, 3.5, 5, 5.5, succinate for pH 4, 4.5, MES for pH 6, 6.5, MOPS for pH 7, and HEPES for pH 8. The uptake reaction was stopped with Dowex-NMG columns, and liposomes were eluted and counted as above.

Use of thiol reagents

MTSES or MTSEA was freshly prepared by dissolving the reagent in ice-cold water just before use. S26C-AdiC was treated for 30 min at room temperature in detergent solution (5 mM DM, 100 mM NaCl, 25 mM tris-HCl, pH 7.5) with 0.5–1 mM reagent, or with 1–5 mM when in liposomes suspended in RB, pH 5.5 (Fig. S2). (For reasons we do not understand, arginine did not lower rate of MTS reaction with the substituted cysteine residue.) Stock aqueous solutions of TCEP (0.6 M, pH 5.5) were kept at 4 °C for up to 1 month. 20 mM stock solutions of fluorescein-maleimide in DMSO were kept at –20 °C in the dark for no more than two weeks.

For labeling of S26C-AdiC in liposomes with fluorescein, EPL liposomes were prepared as usual, and the exposed His-tags were removed by thrombin (0.01 U for a 50-μL liposome sample, 90 min, room temperature). After adding 100 μM phenylmethylsulfonyl fluoride (PMSF) to stop proteolysis, 5 mM MTSES or 1 mM MTSEA + 20 mM TCEP was added, and after the desired time samples were spun through G50 columns equilibrated with 150 mM KCl, 25 mM MOPS, pH 7 to remove thiol reagents. (Samples containing TCEP were spun through G-50 columns twice to ensure complete removal of the reductant.) Fluorescein-maleimide (2 mM) was then added to the liposomes to label remaining free cysteine, and samples were run on 15% SDS-PAGE gels.

Synthesis of ¹⁴C-agmatine

¹⁴C-agmatine was produced by enzymatic decarboxylation of ¹⁴C-arginine. A pT7 expression vector carrying the gene encoding speA, a pyridoxal phosphate (PLP)-dependent arginine decarboxylase, was generously provided by Dr. Yu Ding (10). The plasmid was transformed into BL21 (DE3) cells, which were grown in Terrific Broth at 37 °C to A₅₅₀ ~1 and induced with 1 mM isopropyl α-D-1-thiogalactopyranoside (IPTG) at 25 °C for 4 h. Cells from a 1-L culture were disrupted in 100 mL of 100 mM NaCl, 50 mM tris-HCl, pH 8 in the presence of protease inhibitors (1 mM PMSF, 1 μg/mL leupeptin/pepstatin) and centrifuged at 30,000 g for 25 min. The supernatant was loaded at 1 mL/min onto an 8-mL Ni affinity column equilibrated with wash buffer (WB, 100 mM NaCl, 25 mM tris-HCl, pH 7.5). The column was washed successively with 40 mM and 400 mM imidazole in WB to elute nonspecifically bound protein and speA decarboxylase, respectively. The protein was concentrated to 20 mg/mL and stored at –80 °C with 3 mM DTT and 5% glycerol supplemented. Final yield of speA was ~200 mg/L culture.

To synthesize ¹⁴C-agmatine, 100 μCi ¹⁴C-arginine dissolved in 1 mL of 2% ethanol was mixed with 20 μg speA and 1 mL 100 mM NaCl, 50 μM PLP, 2 mM MgCl₂, 2.5 mM MES, pH 6. After 2 hr at room temperature, the mixture was boiled for 20 min, dried under N₂, and resuspended in 50% ethanol twice to evaporate ¹⁴CO₂. The final preparation of ¹⁴C-agmatine was stored in 2% ethanol at –20 °C. The purity of the preparation was confirmed by high pressure liquid chromatography on a C18 column after derivatization, as described (4).

RESULTS

The orientation of membrane proteins incorporated into biochemically defined lipid membranes can be affected by the method used for reconstitution as well as molecular features specific to the protein. Denoting protein whose extracellular side faces outside of

the liposome as "outside-out", and proteins in the opposite orientation "inside-out," we sought to assess these two possible orientations in AdiC-reconstituted liposomes (Fig. 1B). To this end, proteoliposomes carrying WT AdiC with an N-terminal hexahistidine (H6) tag were incubated with thrombin, which cleaves off the H6 tag exclusively from the inside-out population, since the N-terminus of this protein is cytoplasmic (Fig. 1B). Proteolysis was run to completion, and the sample was analyzed with SDS-PAGE. As can be seen in Fig. 1C, thrombin cleavage produces a lower band representing the lighter, H6-removed AdiC protein; over an extended duration of proteolysis, this inside-out AdiC band reaches an intensity roughly equal to that of the uncleaved, outside-out protein. This assay demonstrates that AdiC is randomly oriented in the liposome membranes.

A strategy to orient AdiC in liposome membranes

A fully oriented reconstituted system for AdiC would be achieved if we could inhibit the protein in one orientation completely while leaving the other orientation unaffected. Although no AdiC inhibitor is known, thiol-specific reagents might serve this purpose in a properly cysteine-substituted transporter. An appropriate design for cysteine substitution should satisfy three conditions. First, the mutation should have limited functional impact, so as to faithfully model wildtype behavior. Second, cysteine modification should lead to complete elimination of functional activity, so that the modified protein would not generate any contaminating signal for transport or binding measurements. Third, the substituted cysteine should be accessible to thiol reagents from only one side of the protein to ensure that only one of the two orientations is subject to modification from a particular side of the membrane.

Guided by crystal structures of arginine-occupied AdiC, we chose Ser26 for cysteine mutation (S26C). This residue, located at the arginine binding site (Fig. 2), interacts with arginine in both "extracellular-open" and "extracellular-occluded" conformations of the transporter (8, 9); a bulky thiol adduct here would be expected to block substrate binding and abolish transport function. Since S26 lies close to the extracellular surface and is well-separated from the intracellular side by layers of aromatic residues (Fig. 2A), we also anticipate that thiol-modifying reagents would reach this position only from the protein's extracellular side. A major concern is the functional impact that the mutation might cause, as in the crystal structure the hydroxyl of S26 forms a hydrogen bond with the carboxylate of bound arginine (Fig. 2B), and conventional wisdom suggests that a Ser-to-Cys mutation would significantly reduce arginine affinity of the protein due to diminished binding energy. However, the fact that AdiC also effectively imports agmatine, which lacks a carboxylate, implies that S26 may not be as crucial as inferred from the crystal structure. We were therefore motivated to examine the suitability of the S26C mutation for functional studies.

The S26C mutant: function and inhibition by MTS reagents

The basic functional characteristics of WT AdiC and the S26C mutant were compared as the first step to gauge whether the three criteria above are satisfied. We note that the S26C mutant to which we henceforth refer is constructed on a "C-less" protein that has all 8 native cysteines mutated to preclude background reaction with thiol reagents. Isothermal calorimetry was used to extract equilibrium substrate-binding parameters (Fig. 3A). Titration of arginine in detergent solution produces endothermic signals with both WT and S26C. The binding data are well described by single-site isotherms with similar values (~30 μ M) of K_D for both. Thus, equilibrium binding of arginine to AdiC is not compromised by the S26C substitution.

Transport function for these AdiC variants was assessed by arginine-arginine exchange in liposomes (6). In a typical experiment, 14 C-arginine enters the liposomes and a steady level

is achieved in 5–10 minutes (Fig. 3B). The S26C mutant is virtually identical in arginine uptake to the C-less control (which itself is approximately 10-fold slower than full-cysteine WT transporter). Moreover, the acid-activation of AdiC is preserved in the S26C mutant (Fig 3C). Taken together, these results show that the S26 mutant on its C-less background functionally mirrors WT protein.

According to the second requirement for an oriented system, the S26C protein must lose function entirely upon modification by thiol-directed reagents. We find that arginine binding, as followed by ITC, is completely lost by treating the mutant with MTSEA in detergent solution (Fig. 4A). Transport activity of S26C is also abolished by MTS modification (Fig. 4B), while the C-less control is unaffected (Fig. S3). Moreover, addition of TCEP during the transport reaction re-activates the inhibited protein by reducing the MTS-modified side chain back to cysteine. These results establish that MTS reagents fully inhibit S26C.

MTSES silences outside-out S26C-AdiC

A crucial condition for achieving our purpose here is that during all stages of the transport cycle, the cysteine substitution site must be accessible from only one side of the membrane-embedded protein. To test this possibility, we challenged reconstituted S26C with the membrane-impermeant reagent MTSES, which can act only from the extraliposomal solution (11). Arginine uptake activity was assayed after incubating liposomes with MTSES for various times. The treatment inhibits arginine import, but not fully (Fig. 5A); substantial transport remains resistant to the inhibitor, even after prolonged exposure. Calibration of transport kinetics as a function of protein concentration in the liposomes shows that the MTSES-treated liposomes have about 50% of the activity of untreated liposomes (Fig. 5B), as if MTSES targets only half of the reconstituted protein population. These experiments strongly refute the idea that C26 may be accessed from both sides of the protein during transport; instead, MTSES acts to fully inhibit AdiC in a sided fashion.

We are uncertain, however, as to the absolute orientation of proteins remaining functional after MTSES inhibition. Crystal structures (7–9) suggest that C26 would be accessible only from the extracellular side, but this conjecture requires direct scrutiny. Accordingly, we designed an experiment (Fig. 6A) to identify those proteins that remain unmodified after MTSES treatment of the liposomes. After removing MTSES from the liposome sample, a membrane-permeant fluorescent maleimide is added to label all AdiC proteins that retain a free thiol. Thrombin is also added to remove the H6 tag exclusively from the inside-out protein fraction, which are then easily distinguished from the outside-out proteins by SDS-PAGE. This strategy demonstrates (Fig. 6B) that the inside-out proteins are spared from MTSES modification, as MTSES prevents fluorescent labeling of only the H6-tagged upper band of AdiC. The results establish that MTSES can be used as a sided inhibitor to create a reconstituted system with functional S26C-AdiC proteins all in the inside-out orientation.

Reconstituted AdiC in an outside-out orientation

Kinetic analysis of membrane transport in liposomes is usually carried out by varying substrates, inhibitors, pH, etc in the extraliposomal solution. It would therefore be desirable to supplement the inside-out AdiC system above with proteins reconstituted in the alternative outside-out orientation. This goal may be accomplished by inhibiting all transporters with a membrane-permeant MTS reagent, MTSEA (11), and then rescuing the outside-out proteins with a membrane impermeant disulfide reductant, TCEP (Fig. 7A).

To test the feasibility of this strategy, we inhibited all AdiC in the liposomes with MTSEA and subsequently examined arginine transport activity. No arginine import is detected after

MTSEA treatment, but addition of 20 mM TCEP restores transport to ~50% of the control sample, as expected if the reductant acts exclusively upon the outward-facing C26 adduct (Fig 7B). To confirm this picture, the liposomes were further treated with fluorescein-maleimide and thrombin as above. Since only the upper band becomes fluorescent following TCEP reduction (Fig 7C), we conclude that a combination of MTSEA and TCEP can produce fully oriented outside-out AdiC transporters.

Kinetic analysis of substrate transport

Now with sided reconstituted systems available, the stage is set for exploring the substrate specificity for the two sides of AdiC. Arginine in the external solution was varied, keeping intraliposomal arginine fixed at a saturating concentration, and initial rates of uptake were measured in outside-out and inside-out orientations (Fig. 8). Arginine uptake follows Michaelis-Menten kinetics in both cases, with K_m of ~100 μM and ~50 μM for the cytoplasmic and extracellular sides, respectively, and similar V_{max} values for both orientations, on the order of 0.1 s^{-1} . Similar experiments with ^{14}C -agmatine uptake were also conducted (Fig. 8C), yielding K_m and V_{max} similar to those for arginine, as summarized in Table 1.

The physiological role of AdiC to counter acidification of cytosol demands that AdiC transports only the deprotonated carboxylate form of arginine (Arg^+), a minor species at pH below 2.3 (6). We have shown previously that argininamide (ArgNH_2), an analogue of protonated Arg^{+2} , is a poor transport substrate compared to Arg^+ (6). Here, we revisit this issue in an oriented system, using ArgNH_2 as a competitor for ^{14}C -arginine-arginine exchange. Arginine uptake is slowed by ArgNH_2 in either orientation according to simple competitive inhibition (Fig. 9), but the competitor is 5-fold less effective on the extracellular vs intracellular side of AdiC (Table 1). This result conforms to the biological context, since it is the low-pH extracellular side of the transporter that must distinguish Arg^+ from Arg^{+2} ; this selectivity is unimportant in the cytoplasm, where Arg^{+2} is negligible because intracellular pH never falls below pH 4.5 (12, 13).

Sided pH-sensitivity of AdiC

AdiC-mediated transport is stimulated by low pH (Fig. 3C), as is unsurprising for a protein whose biological task is performed in a strongly acidic environment. To determine the side of AdiC where pH is sensed, we varied pH for one side of the protein while fixing the other side at pH 5.5. For extracellular variation, arginine transport is low around neutrality and increases ~30-fold to a plateau as pH is lowered from 8 to 3 (Fig. 10A). This finding makes physiological sense, as it is the extracellular side of AdiC that directly experiences strong acidification in the stomach. Cytoplasmic pH also drops during extreme acid challenge, to as low as pH 4.5 but not lower (12, 13). This biological response is reprised in the bell-shaped dependence of transport on cytoplasmic pH (Fig. 10B), which shows a 3-fold increase in activity from neutrality to a maximum near pH 5, followed by a decrease as pH is further lowered, a condition that the acid-resisting cytoplasm never experiences. We therefore suppose that each side of AdiC carries its own pH sensor, each tuned to the conditions prevailing during the arginine-dependent XAR response.

DISCUSSION

AdiC belongs to the amino acid-polyamine-organocation (APC) transporter superfamily, whose members appear throughout the biological world. APC transporters mediate a panoply of biological tasks, such as supplying amino acids for metabolism, arginine for nitric oxide synthesis, and headgroups such as choline, ethanolamine, and inositol for phospholipid synthesis, as well as energizing membranes of certain anaerobic bacteria in the

absence of electron transport. In bacterial XAR, AdiC specifically imports arginine from gastric fluid and exports agmatine along with a "virtual proton" (5, 6) out of the cytosol in each turnover. Specific recognition of extracellular arginine can be understood from x-ray crystal structures of AdiC solved in two arginine-bound states: extracellular-open (9) and extracellular-occluded (8). In these structures, the aromatic side chain of Trp293 appears to stabilize arginine binding by a cation- π interaction with the substrate's guanidinium group. Mutagenesis of a variety of APC transporters have identified aromatic interactions as crucial for substrate binding, and indeed mutations of Trp293 in AdiC itself lead to a complete loss of transport activity (6).

A less understood molecular interaction in AdiC's crystal structures is a hydrogen bond between the α -carboxylate of arginine and the hydroxyl group of Ser26, a residue conserved among APC virtual proton pump exchangers (7). Although it is natural to imagine that this interaction would provide significant binding energy for extracellular amino acids, we find with some surprise that Cys (Fig. 3) or Ala (Fig. S4) substitutions at Ser26 do not undermine arginine transport. Viewed from an evolutionary perspective, however, these results appear less puzzling, since in the stomach, where amino acids are available, the external-facing conformation of AdiC faces no evolutionary pressure to differentiate amino acids from substrates with other chemical groups attached to the α -carbon. A vivid example seen here is that agmatine, which lacks the α -carboxylate, has a similar extracellular transport K_m ($\sim 50 \mu\text{M}$) as arginine.

No AdiC structure has yet been solved in the cytoplasmic-open conformation. With the sided system developed here, we may begin to gain insight into ligand binding and specificity for AdiC's intracellular side. Kinetic analysis reveals that arginine and agmatine have a similar K_m ($\sim 100 \mu\text{M}$) for this side of the protein, a result that appears surprising at first glance, as transport of arginine from the cytoplasm would produce a futile cycle useless for acid resistance, and one might therefore expect intracellular selectivity for agmatine. We should remember, however, that cytoplasmic arginine is kept low by robust decarboxylation and thus presents no problem as a cytoplasmic competitor for agmatine.

In the gastric fluid, the two sides of AdiC operate under very different conditions. Extracellular pH can fall as low as 1.5, while cytoplasmic pH is maintained in the range 4.5–5.5 by the XAR response (13). Therefore, the two sides of AdiC must deal with distinct environmental challenges. With a pK_a of 2.3, arginine's carboxylate presents a problem of molecular recognition, since the outward-facing conformation must select the minor, deprotonated α -carboxylate form, Arg^+ , over the preponderant protonated form, Arg^{2+} , to achieve acid resistance (6). Previous work showed that AdiC transports ArgNH_2 , a mimic of Arg^{2+} , with substantially lower efficiency than Arg^+ , but the sidedness of this selectivity could not be determined because of the random protein orientation in the liposomes (6). Now with the oriented system, we find that extracellular ArgNH_2 is substantially less effective than intracellular as a competitive inhibitor of Arg^+ transport. In other words (assuming that ArgNH_2 serves as a valid analogue of Arg^{2+}), the outward-facing conformation is more sensitive than the inward-facing to the protonation state of arginine, a circumstance resonant with the biological imperatives that AdiC must satisfy.

Previous work (6) established that AdiC transport activity is stimulated by acidification, but the random protein orientation in that work made it impossible to evaluate the sidedness of this effect. Now with the oriented system, we find that both sides of the protein sense pH, each with its own characteristic pH profile. The major, extracellular pH-sensor leads to ~ 30 -fold stimulation upon acidification from neutrality, while intracellular acidification produces a biphasic response with 3-fold stimulation followed by inhibition below pH 4. We do not currently understand the molecular basis for this pH-dependent transport activity, but the

differing pH profiles for the two sides of the protein imply that at least two pH sensors are involved, one for each side of the membrane. This situation makes biological sense. Under non-stressed conditions, near neutrality on both sides of the bacterial inner membrane, AdiC transport activity is low, and only upon extracellular acidification does the transporter spring into action. We estimate that the two sensors working together in response to typical acid stress conditions - extracellular and cytoplasmic pH of 3 and 5.5, respectively - accelerate the rate of virtual proton pumping ~50-fold (Fig. S5). It is also notable that the bell-shaped cytoplasmic pH profile for transport is similar in shape to the pH-dependence of the acid-activated arginine decarboxylase AdiA (14, 15) - a satisfying example of a sophisticated, multi-protein system in which all components are poised to respond to a stress condition in a coordinated way.

Our results also offer a cautionary note regarding the logic sometimes mustered to argue for H⁺-coupled mechanisms in transport proteins. For instance, in a recent description of the structure and mechanism of ApcT, a wide-spectrum APC amino acid transporter, it was shown (16) that substrate uptake is increased ~3-fold in the presence of a pH gradient (pH 4-outside /pH 7-inside), as compared with symmetrical pH 4 conditions. This result was taken to mean that a proton is co-transported with the amino acid, i.e., that ApcT is a H⁺-coupled amino acid symporter. However, as shown here, AdiC, which does not co-transport protons (6), is also stimulated by a similar pH gradient (pH 3-outside / 5.5-inside, vs symmetrical pH 5.5). Thus, the type of evidence adduced to identify ApcT as a H⁺-coupled symporter neither supports nor refutes that conclusion.

In this study, we developed an oriented reconstituted system for AdiC and used it to extract sided kinetic parameters for substrate transport and other functional properties of AdiC. Many unresolved problems and ambiguities concerning this protein remain for future examination. For example, the precise role of Ser26 in substrate selectivity is still in question, despite the implication from crystal structures alone, of a strong H-bond donated to substrate by this side chain. In addition, the specific influences of pH on substrate transport have not yet been dissected mechanistically, nor have the protein's pH sensors been identified. The sided system described here will be a useful tool for future approaches to these problems.

Supplementary Material

Refer to Web version on PubMed Central for supplementary material.

Acknowledgments

We thank Dr. Ludmila Kolmakova-Partensky for help with some of the early experiments reported here and Dr. Yu Ding, Fudan Univ, for providing the speA expression plasmid. This work was supported in part by NIH grant #GM-089688.

Funding: NIH grant # GM-089688

References

1. Castanie-Cornet MP, Penfound TA, Smith D, Elliott JF, Foster JW. Control of acid resistance in *Escherichia coli*. *J Bacteriol*. 1999; 181:3525–3535. [PubMed: 10348866]
2. Foster JW. *Escherichia coli* acid resistance: tales of an amateur acidophile. *Nat Rev Microbiol*. 2004; 2:898–907. [PubMed: 15494746]
3. Gong S, Richard H, Foster JW. YjdE (AdiC) is the arginine:agmatine antiporter essential for arginine-dependent acid resistance in *Escherichia coli*. *J Bacteriol*. 2003; 185:4402–4409. [PubMed: 12867448]

4. Iyer R, Williams C, Miller C. Arginine-agmatine antiporter in extreme acid resistance in *Escherichia coli*. *J Bacteriol*. 2003; 185:6556–6561. [PubMed: 14594828]
5. Maloney PC. The molecular and cell biology of anion transport by bacteria. *Bioessays*. 1992; 14:757–762. [PubMed: 1365888]
6. Fang Y, Kolmakova-Partensky L, Miller C. A bacterial arginine-agmatine exchange transporter involved in extreme Acid resistance. *J Biol Chem*. 2007; 282:176–182. [PubMed: 17099215]
7. Fang Y, Jayaram H, Shane T, Kolmakova-Partensky L, Wu F, Williams C, Xiong Y, Miller C. Structure of a prokaryotic virtual proton pump at 3.2 Å resolution. *Nature*. 2009; 460:1040–1043. [PubMed: 19578361]
8. Gao X, Zhou L, Jiao X, Lu F, Yan C, Zeng X, Wang J, Shi Y. Mechanism of substrate recognition and transport by an amino acid antiporter. *Nature*. 2010; 463:828–832. [PubMed: 20090677]
9. Kowalczyk L, Ratera M, Paladino A, Bartoccioni P, Errasti-Murugarren E, Valencia E, Portella G, Bial S, Zorzano A, Fita I, Orozco M, Carpeta X, Vazquez-Ibar JL, Palacin M. Molecular basis of substrate-induced permeation by an amino acid antiporter. *Proc Natl Acad Sci U S A*. 2011; 108:3935–3940. [PubMed: 21368142]
10. Song J, Zhou C, Liu R, Wu X, Wu D, Hu X, Ding Y. Expression and purification of recombinant arginine decarboxylase (speA) from *Escherichia coli*. *Molecular Biology Reports*. 2010; 37:1823–1829.
11. Holmgren M, Liu Y, Xu Y, Yellen G. On the use of thiol-modifying agents to determine channel topology. *Neuropharmacology*. 1996; 35:797–804. [PubMed: 8938712]
12. Foster JW, Hall HK. Inducible pH homeostasis and the acid tolerance response of *Salmonella typhimurium*. *J Bacteriol*. 1991; 173:5129–5135. [PubMed: 1650345]
13. Richard H, Foster JW. *Escherichia coli* glutamate- and arginine-dependent acid resistance systems increase internal pH and reverse transmembrane potential. *J Bacteriol*. 2004; 186:6032–6041. [PubMed: 15342572]
14. Blethen SL, Boeker EA, Snell EE. Arginine decarboxylase from *Escherichia coli*Purification and specificity for substrates and coenzyme. *J Biol Chem*. 1968; 243:1671–1677. [PubMed: 4870599]
15. Kanjee U, Gutsche I, Ramachandran S, Houry WA. The enzymatic activities of the *Escherichia coli* basic aliphatic amino acid decarboxylases exhibit a pH zone of inhibition. *Biochemistry*. 2011; 50:9388–9398. [PubMed: 21957966]
16. Shaffer PL, Goehring A, Shankaranarayanan A, Gouaux E. Structure and mechanism of a Na^+ -independent amino acid transporter. *Science*. 2009; 325:1010–1014. [PubMed: 19608859]

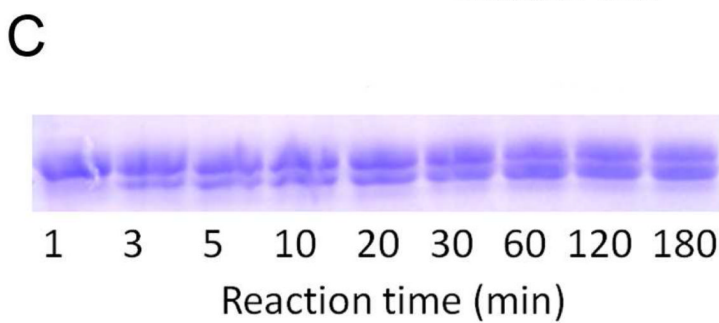
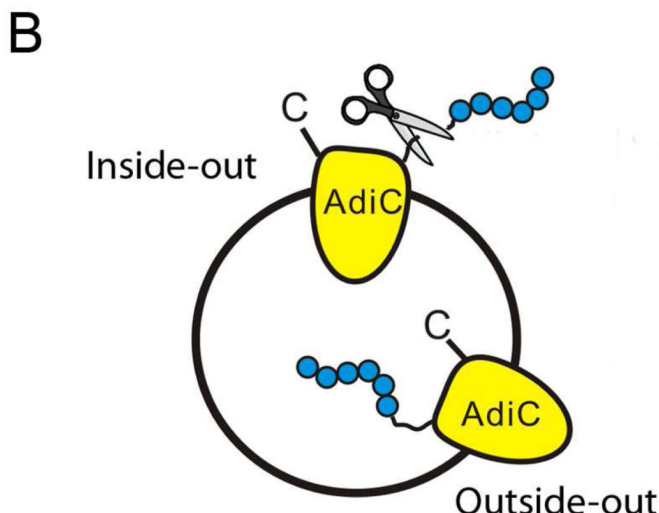
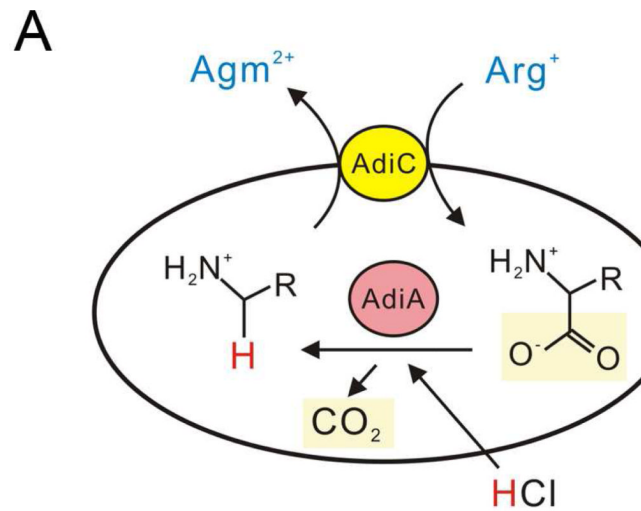


Fig. 1. Orientation of AdiC in liposome membranes

A. Mechanism of the arginine-dependent XAR system. B. AdiC in inside-out and outside-out orientations. N-terminal H6 tag (blue circles) of the inside-out protein, exposed to the outside of the liposome, is susceptible to thrombin cleavage (scissors). C. Determination of AdiC orientation. Thrombin (0.01 U) was added to 100- μ L liposome aliquots (10 μ g AdiC/mg lipid). At the indicated time points, proteolysis was stopped by 100 μ M PMSF, and samples were analyzed by SDS-PAGE.

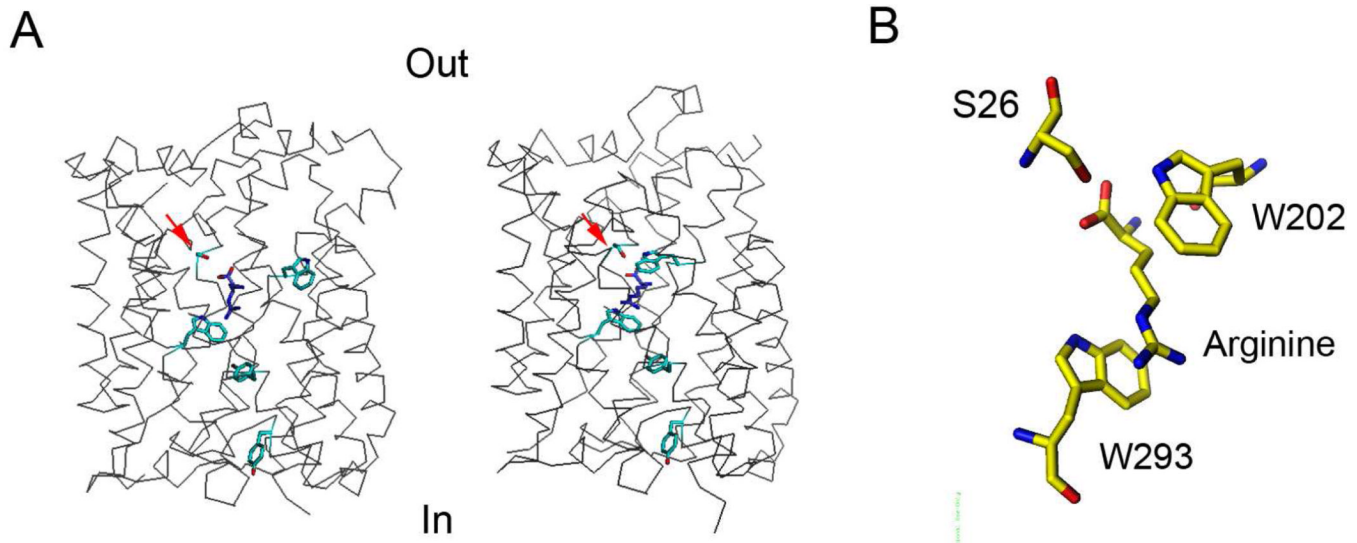


Fig. 2. Ser26 in crystal structures of AdiC

A. The extracellular-open (left, PDB code: 3OB6) and extracellular-occluded (right, PDB code: 3L1L) states of AdiC. Red arrows indicate the position of Ser26, which interacts directly with arginine (purple) and is separated from the cytoplasmic side by protein containing layers of aromatic residues. B. The arginine binding site of the extracellular-occluded state. The guanidinium side chain is sandwiched between Trp202 and Trp293, and the α -carboxylate forms a hydrogen bond with the hydroxyl of Ser26.

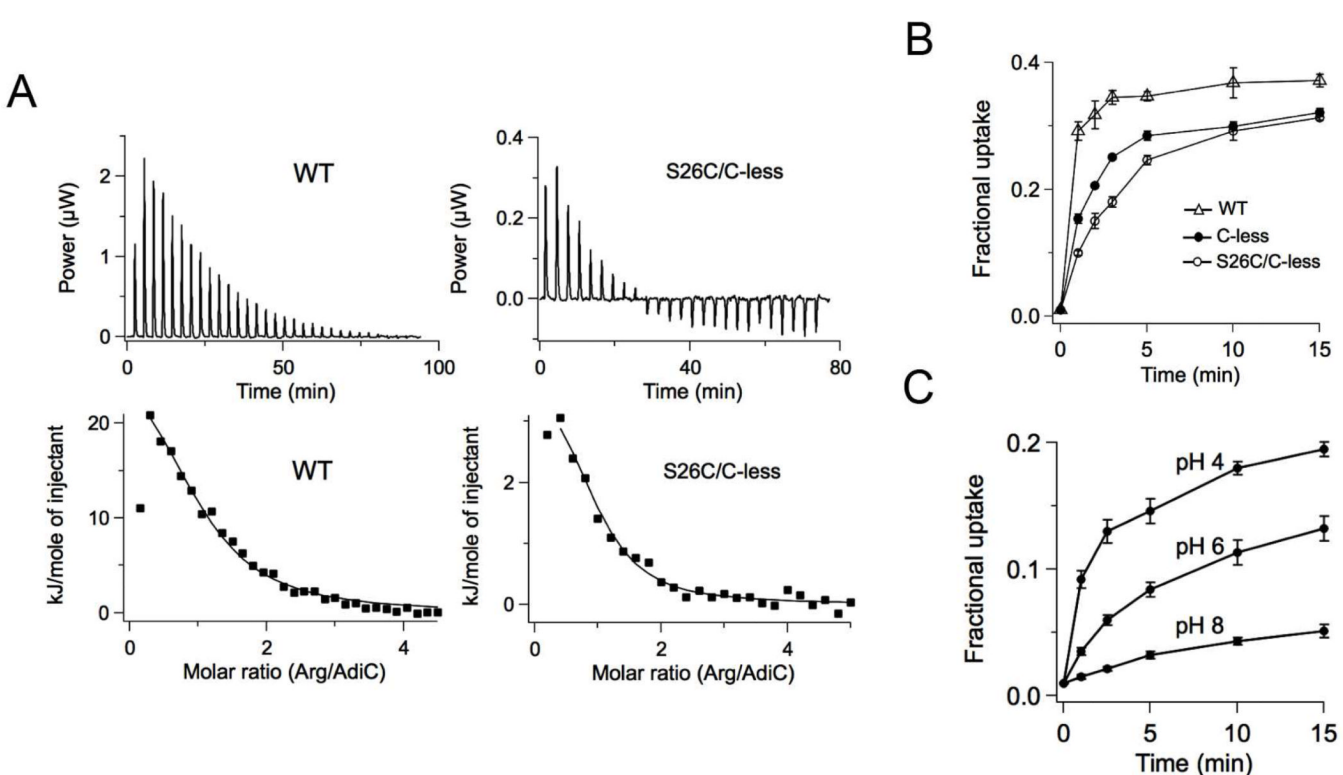
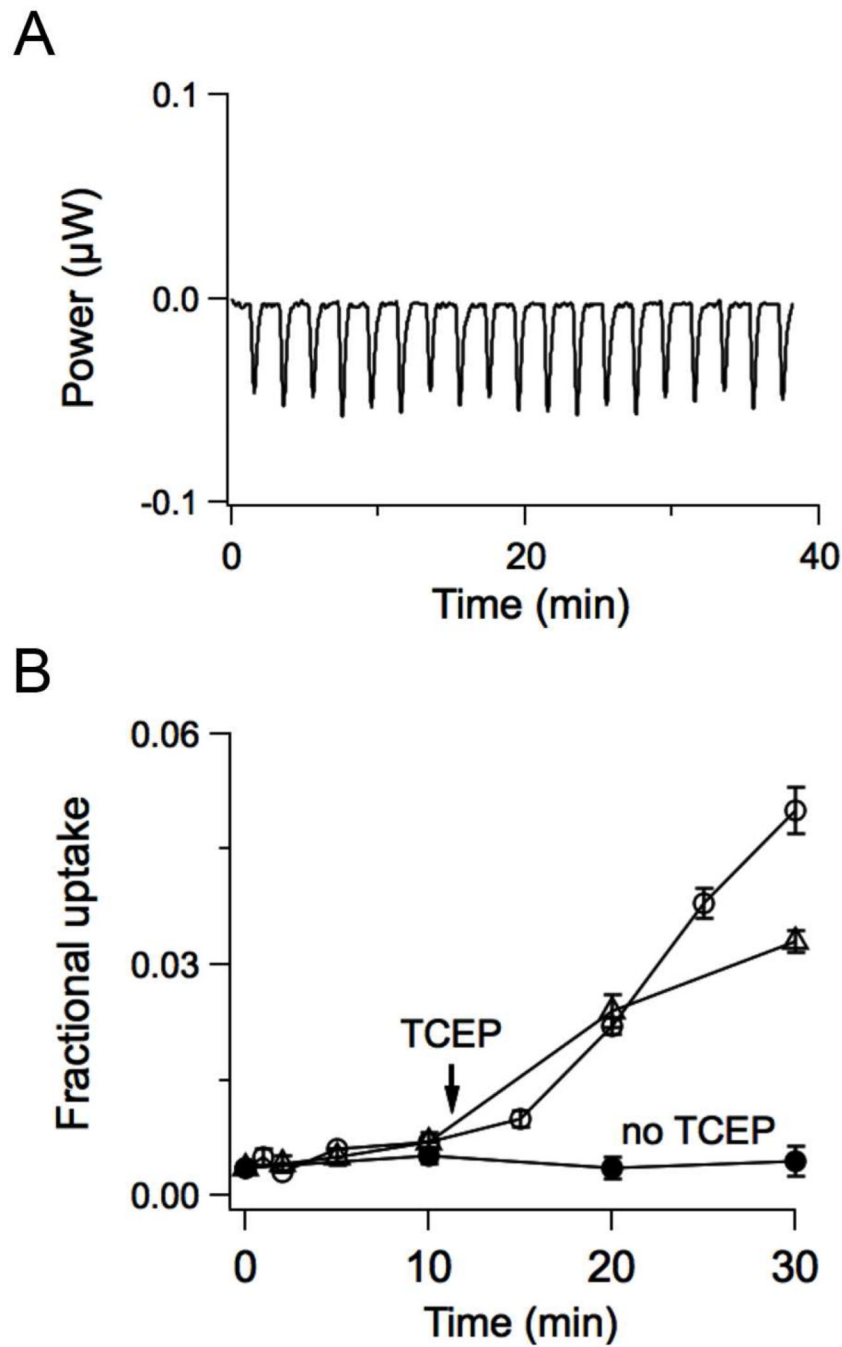


Fig. 3. Functional impact of the S26C mutation

A. Equilibrium binding of arginine to WT and the S26C mutant. ITC data (upper) were fit with single-site isotherms (lower), yielding the following parameters. WT (n = 4): $K_D = 32.2 \mu\text{M}$, $\Delta H^\circ = 6.4 \pm 0.3 \text{ kcal/mol}$, $\Delta G^\circ = -6.2 \pm 0.1 \text{ kcal/mol}$, and $\Delta S^\circ = 42.1 \text{ cal/mol-K}$. S26C (n=3): $K_D = 22 \pm 2 \mu\text{M}$, $\Delta H^\circ = 3.1 \pm 0.4 \text{ kcal/mol}$, $\Delta G^\circ = -6.3 \pm 0.1 \text{ kcal/mol}$, and $\Delta S^\circ = 32.1 \text{ cal/mol-K}$. B. Arginine transport by WT and mutant AdiC. Uptake timecourse of ^{14}C -arginine was determined with indicated AdiC constructs reconstituted at 10 $\mu\text{g}/\text{mg}$ lipid). C. pH-dependent transport activity of S26C. Uptake timecourses were performed at the indicated symmetrical pH with protein reconstituted at 5 $\mu\text{g}/\text{mg}$.

**Fig. 4. Inhibition of S26C-AdiC by MTS reagents**

A. An illustrative ITC experiment with arginine titrated into a sample containing 150 μ M MTSEA-modified S26C protein showing no binding signal. B. Effects of MTS reagents on transport activity of S26C-AdiC. S26C protein treated with 5 mM MTSEA (open or closed circles) or MTSES (open triangles) in detergent was reconstituted into liposomes at 10 μ g/mg lipid, and arginine uptake was measured over a 30-min period. At 11 min into the timecourse, 20 mM TCEP was added (arrow), except to the control samples (closed circles).

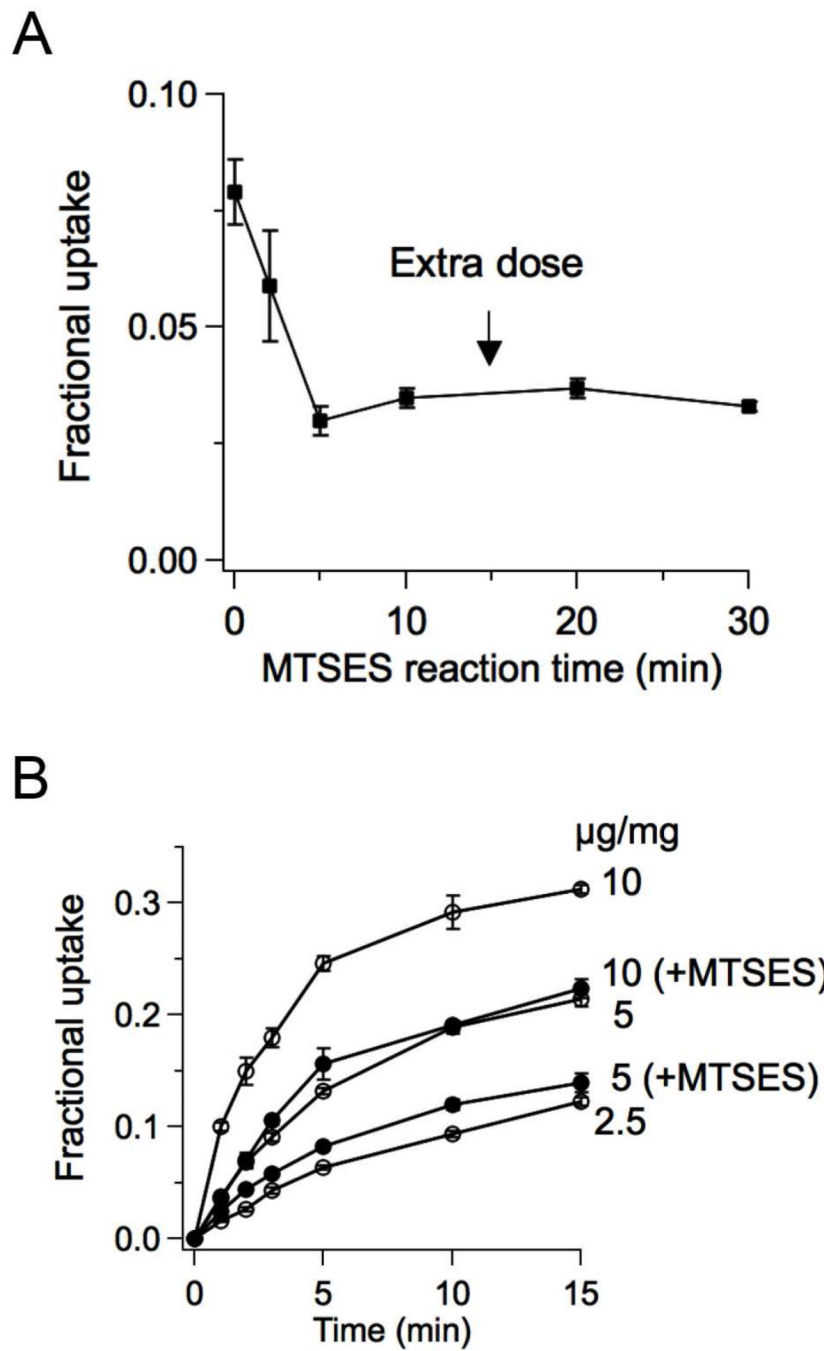


Fig. 5. Sided inhibition of S26C-AdiC by MTSES

A. Timecourse of inhibition by MTSES. Liposomes reconstituted with S26C-AdiC (10 $\mu\text{g}/\text{mg}$ lipid) was exposed to 5 mM MTSES. At the indicated times, a 100- μL sample was spun through G50 columns to remove MTSES, and a 1-min arginine uptake assay was performed. For samples with more than 15 min MTSES exposures, an extra dose of 5 mM MTSES (arrow) was added to compensate the loss of MTSES due to hydrolysis. B. Calibration of MTSES inhibition. Arginine uptake timecourses were determined using liposomes reconstituted with S26C-AdiC at 2.5, 5, or 10 μg protein/mg lipid, as indicated. Closed circles: liposome pre-treated with 5 mM MTSES for 30 min. Open circles, untreated control liposomes.

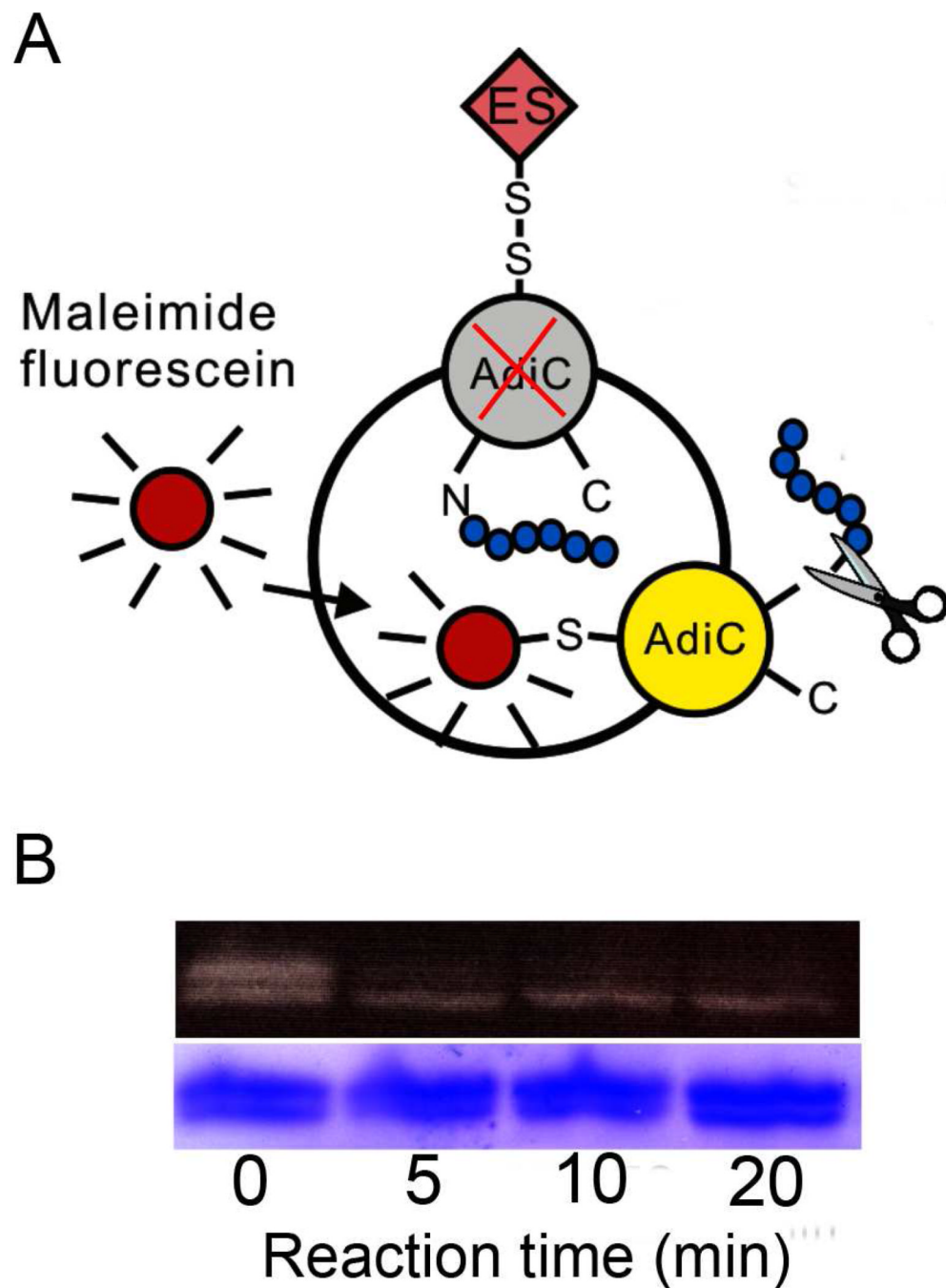


Fig. 6. Inside-out orientation of AdiC in MTSES-treated liposomes

A. Strategy to create an inside-out system. B. Fluorescein labeling of AdiC in MTSES-treated liposomes. 5 mM MTSES was added to 100- μ L liposome samples (10 μ g protein/mg lipid) and subsequently removed by spinning the samples through G-50 columns at indicated times. Unmodified proteins were then labeled to completion with 2 mM fluorescein maleimide and cleaved with thrombin. Samples were analyzed by SDS-PAGE and visualized by fluorescence (upper panel) or coomassie staining (lower panel).

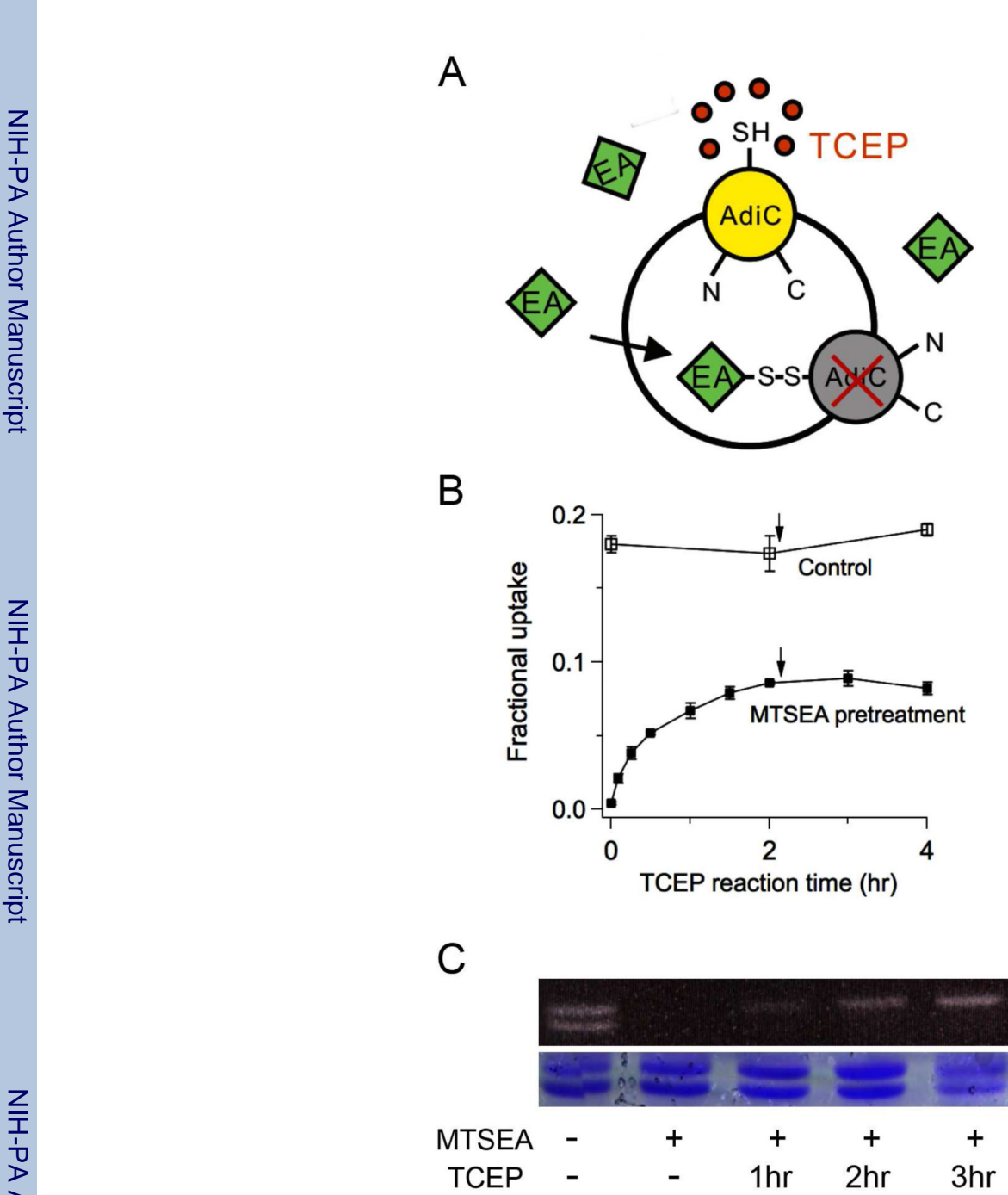


Fig. 7. Outside-out orientation of AdiC in MTSEA/TCEP-treated liposomes

A. Strategy to create an outside-out system. B. Arginine transport rescued by TCEP. S26C-reconstituted liposomes (10 µg/mg) with (closed square) or without (open square) 30-min exposure to 1 mM MTSEA were treated with 20 mM TCEP for various times, with an extra dose of 20 mM added at 2 hr (arrow). After removing TCEP, a 3-min arginine uptake was measured to ascertain recovery of transport function. C. Fluorescein-maleimide labeling after indicated MTSEA/TCEP treatment. After labeling, samples were analyzed by SDS-PAGE as in Fig 6.

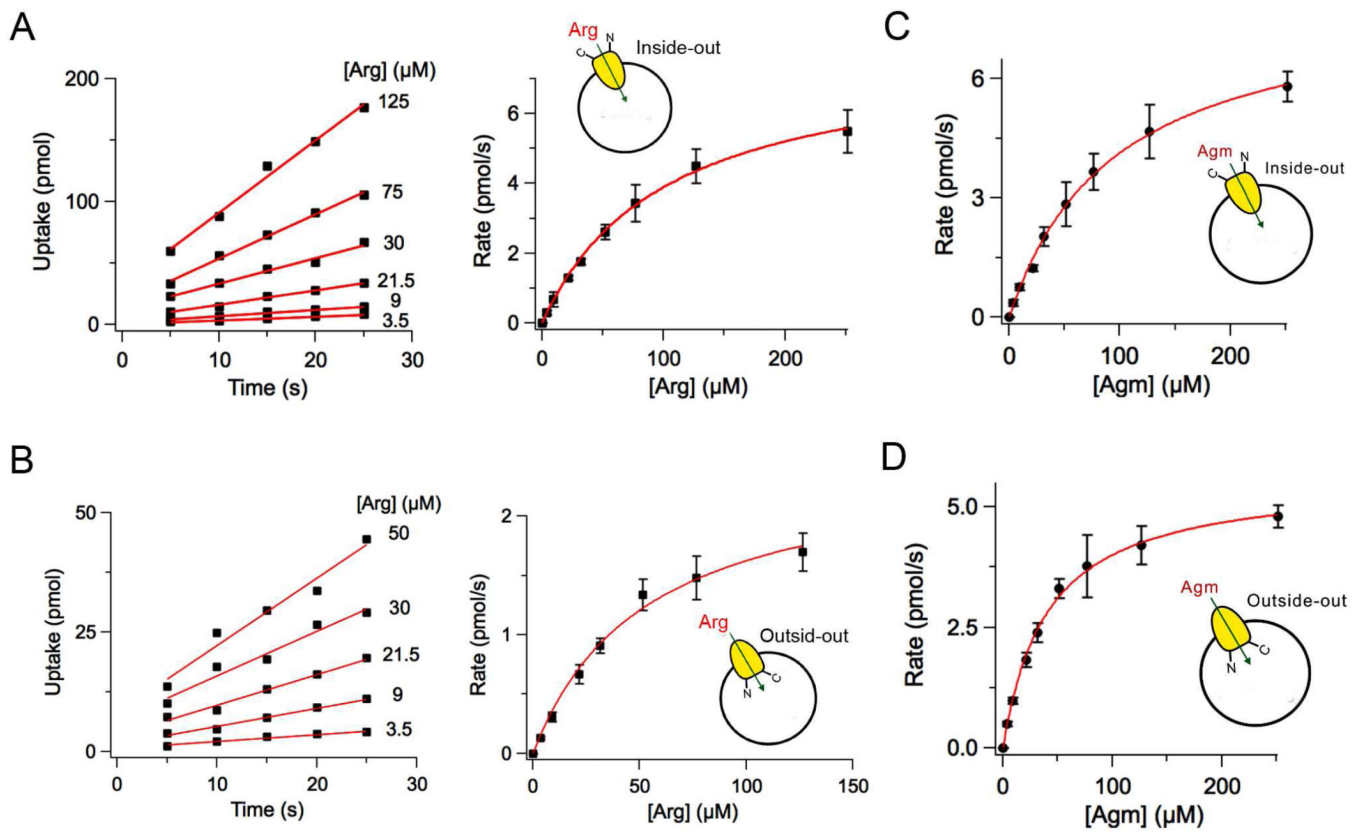
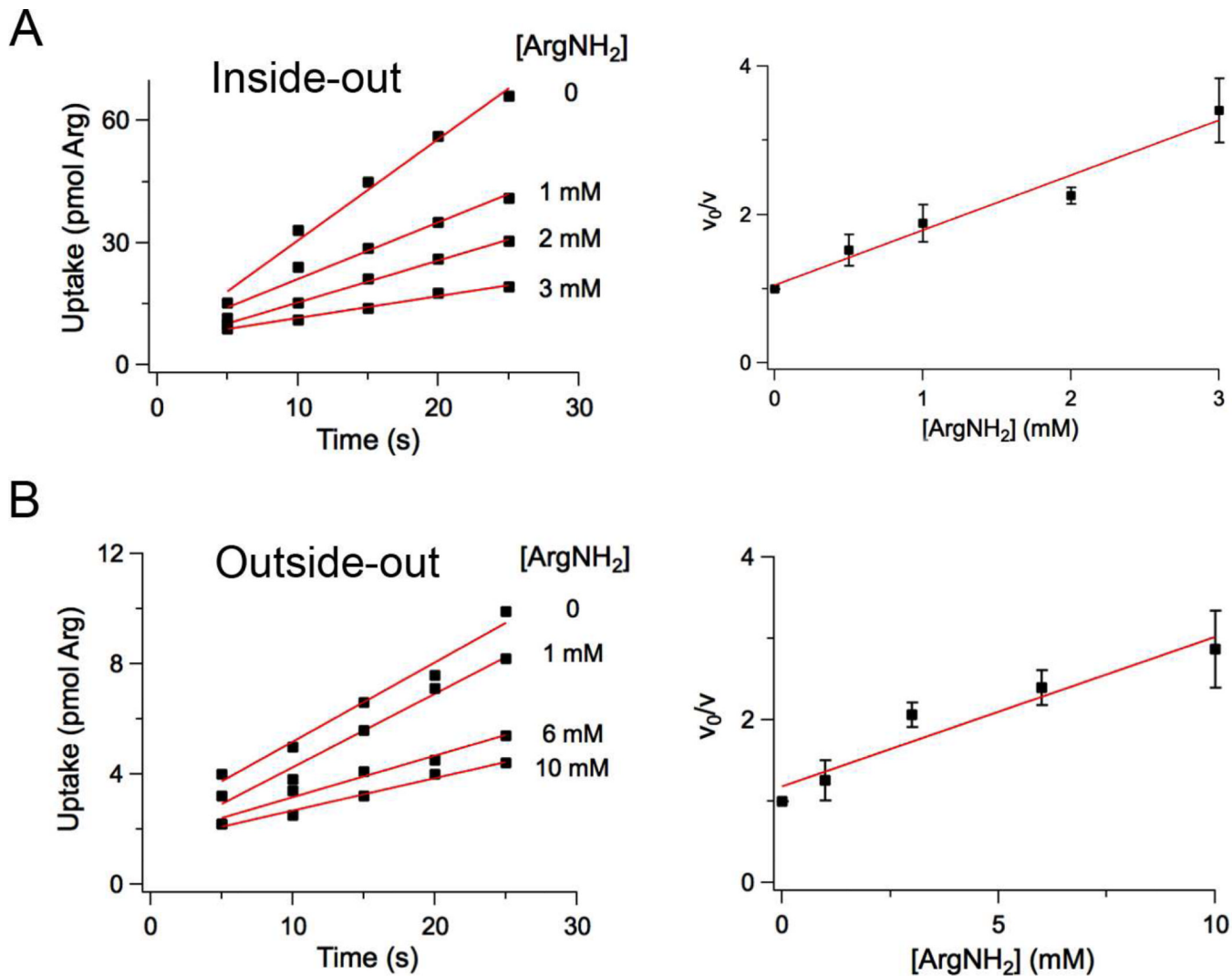


Fig. 8. Sided kinetic analysis of substrate transport

A, B. Kinetic analysis of arginine uptake. ^{14}C -arginine uptake into liposomes loaded with 5 mM arginine and carrying inside-out (A) or outside-out (B) AdiC (10 $\mu\text{g}/\text{mg}$ lipid) was examined as a function of the indicated external arginine concentrations. Left panels: illustrative initial-rate data over a 25-sec timecourse in a single run in which each sample contains 6.5 μg of AdiC. Center panels: rates plotted against arginine concentration were fit to Michaelis-Menten model (solid curves), with parameters summarized in Table 1; each point represents mean \pm s.e. from 3–5 separate runs. C–D. Kinetic analysis of ^{14}C -agmatine uptake. Experimental conditions were as in A, B, except that uptake of agmatine was followed in inside-out (C) or outside-out (D) AdiC liposomes.

**Fig. 9. ArgNH₂ inhibition of arginine uptake**

Inside-out (A) or outside-out (B) liposomes were prepared as in Fig 8, and ¹⁴C-arginine uptake was measured in the presence of indicated external concentrations of ArgNH₂. Left panels: initial rate timecourses. Right panels: reciprocal plots of rate relative to its value in the absence of ArgNH₂(v₀/v). Lines are fits to Michaelis-Menten kinetics with parameters reported in Table 1.

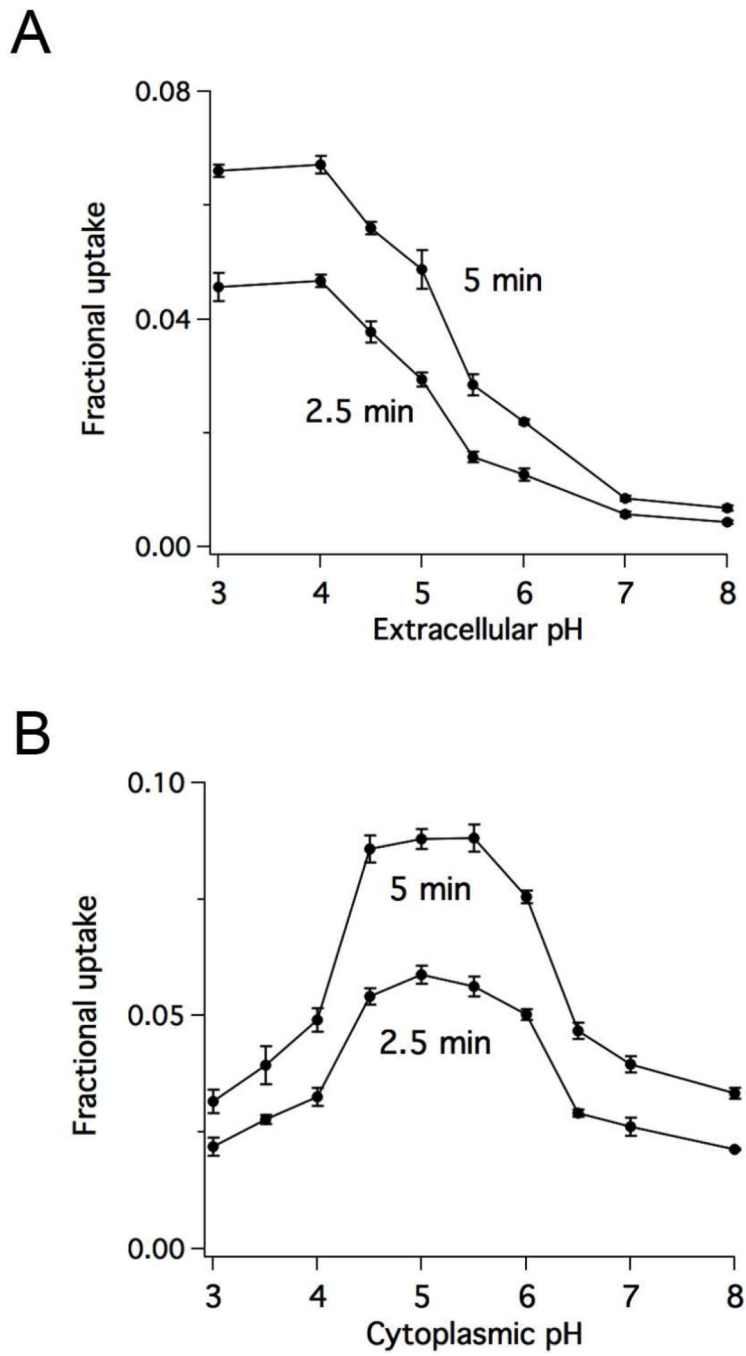


Fig. 10. Distinct pH sensitivities of the two sides of AdiC

Liposomes with AdiC in outside-out (A) or inside-out (B) orientations were prepared with internal of pH 5.5. Arginine uptake was performed at the indicated external pH, for either 2.5 or 5 min.

Michaelis-Menten parameters for arginine, agmatine, and argininamide.

Table 1

AdiC orientation	Arginine	Agmatine	ArgNH_2	K_m (μM)	V_{max} (pmol/s)	k_{cat} (s^{-1})	V_{max} (pmol/s)	k_{cat} (s^{-1})	K_i (mM)
Inside-out	101	7.8	0.12	96	8.1	0.12	8.1	0.12	1.1
Outside-out	52	2.5	0.04	40	5.6	0.08	5.2	0.08	5.2

Parameters reported are from the least-squares fits shown in Fig 8 and 9.